In silico prototype of a human lung with a single airway to predict particle deposition

Ana Fernández-Tena[1], Raúl Barrio-Perotti[2], Eduardo Blanco-Marigorta[3] and Adrián Pandal-Blanco[4]

[1] Corresponding author, Facultad de Enfermería, Universidad de Oviedo, 33203 Gijón, Spain. E-mail tenaana@uniovi.es. ORCID 0000-0002-5944-4023.
[2] Departamento de Energía, Universidad de Oviedo, 33204 Gijón, Spain. E-mail barrioraul@uniovi.es. ORCID 0000-0002-2285-095X.
[3] Departamento de Energía, Universidad de Oviedo, 33204 Gijón, Spain. E-mail eblanco@uniovi.es. ORCID 0000-0003-3290-201X.
[4] Departamento de Energía, Universidad de Oviedo, 33204 Gijón, Spain. E-mail pandaladrian@uniovi.es. ORCID 0000-0001-6006-2199.

Abstract

Background: experimental analyses of the flow of drug particles inside the human lung usually require that the patient be exposed to radiation and also of expensive equipment that often lack of enough accuracy. Numerical calculations based on CFD (Computational Fluid Dynamics) have been proven to be a valuable tool to analyze flows in diverse applications.

Methods: the complexity of the human lung disallows running calculations on complete lung models due to the large number of cells that would be required. In this work, using a proprietary methodology, particle deposition in the lung is simulated by reducing its multiple branches to a single path.

Results: the tested flow rates were 18, 30 and 75 L min^{-1}, which are equivalent to different respiratory rates varying from light activity to heavy exercise. Most of the particles are accumulated in the upper airways, mainly at the mouth and also at the confluence of the larynx and the trachea (epiglottis), while the remaining particles travel across the lung. The reported procedure allowed simulating the operation of the entire lung by means of a single individual path.

Conclusions: the obtained calculations are in good agreement with the experimental results found in the technical literature, thus showing that the model can provide a realistic description of the lung operation while avoiding high computational costs. Moreover, the calculations suggest that particle sizes above 15 μm and inspiratory flows higher than 30 L min^{-1} must be avoided in order to allow drug particles to reach the lower airways.

Keywords: Boundary condition; In-silico; CFD calculations; Particle deposition; Single airway

1. Introduction

Air pollution is an aspect of the environmental problems that is a direct consequence of our current model of development [1]. Several studies have associated air pollution with a wide range of health effects. However, since the mixture of air contaminants encloses many different substances, it is very complex to relate specific health problems with a particular pollutant [2] because detected effects could result from one or more air pollutants [3–5]. It is well known that these effects are close dependent on pollutant size, since the human body is designed to remove the larger particles and prevent their accumulation in the lungs. The particle size is usually characterized by the Mass Median Aerodynamic Diameter (MMAD), which is defined as the diameter of a particle of mass that is equal to the average particle diameter of a population [6] or, in other words, it represents the diameter of a particle in which 50% of the mass is larger and the other 50% is smaller [7].

The size and shape of the particles are essential factors that condition their deposition in the lungs. In general, it is considered that particles with an MMAD higher than 10 μm are accumulated in the oropharynx, while those ranging between 5 and 10 μm are collected in the central airways. Finally, particles ranging from 0.5 to 5 μm can reach the smaller airways and even the alveoli, where they can move from the lung to the blood stream and other body parts. Nevertheless, particle deposition is not only a process to be avoided. In fact, when drugs are considered instead of pollution particles, its deeper deposition is highly desired. In consequence, it is advisable to use particles with an MMAD between 0.5 and 5 μm, known as the respirable fraction of an aerosol [8], for typical respiratory treatments. Particularly, it is common that aerosolized drug particles show a homogeneous shape while being exceptionally smaller than 1 μm [9].

The chance of particle deposition by collision inside the lung intensifies for a larger size of the particles and also when the inspired flow of air is higher. Additionally, the deposition is also increased for wider angles of the branches and narrower airways [10]. Diseases like bronchitis or asthma may generate bronchoconstriction, inflammation or secretion accumulation, thus changing the lung morphology and reducing the diameter of the airways, which alters the pattern of deposition of aerosolized drugs. A smaller airway diameter increases air speed and generates turbulence at locations where the flow is usually laminar. The airway obstruction also brings about that the air is forced to move towards unobstructed areas, and therefore drug particles would be mostly collected inside healthy areas of the lung [11]. Previous studies [12] demonstrated that the amount of deposition for any particle size increases until the 4th level or generation of the airways as the inspiratory flow also increases. However, the opposite trend was observed at the smaller generations of the airways. This is a consequence of the decrease in the residence time of the particles along the airways for increasing inspiratory flows. Certainly, a minimum inspiratory flow is required to drag the particles towards the bronchial tree, and thus it is crucial to understand the factors that affect the deposition of particles inside the lung in order to improve the mechanisms of drug delivery for the treatment of lung diseases.

Studies of particle deposition inside the lung are quite complex both from the experimental point of view and from numerical approaches such as Computational

Fluid Dynamics (CFD). Advanced imaging techniques (e.g. Single-Photon Emission Computed Tomography, SPECT) are being used recently to carry out experimental measurements, although their performance is limited because they cannot clearly identify the airway level at which particles are deposited. Another experimental solution can be the use of cadavers or laboratory models of lungs [13]. The problem with these methods is that an expensive equipment is usually required in order to visualize the particles and additionally, tests must be performed sequentially. The main advantage of CFD techniques for the research of particle deposition is that any part of the lung can be accessed to visualize the deposition process, without needing of complex laboratory experiments. Furthermore, several cases can be tested at once in parallel since these are non-invasive techniques [14]. When particles are inhaled, the two-phase flow that is established inside the lung, including its dynamic behavior, is influenced by the geometric properties of the particles such as their size and statistical distribution. If the particle motion is chiefly induced by fluid forces (drag, lift, etc.) the particles can be considered as a dispersed phase inside the flow. These particular characteristics must be retained during the CFD model construction.

As it is widely known, the human lung consists of a series of dichotomous branching generations or levels [15, 16], which begin at level 0 (trachea) and finish at level 23 (alveolar sacs). The sector located between levels 0 and 16 is usually referred to as conductive zone, while the interchange area extends between levels 17 to 23, where the pulmonary exchange of oxygen takes place in addition to the air transport. At present, CFD simulations are mostly limited to certain areas of the lung geometry due to the considerable difficulty of assembling an entire model of the lung, being the flow in the lower airways either ignored or modelled by using axisymmetric approximations. This is because of the fact that a full description of the human lung with 23 levels would require nearly 16 million segments, with an estimated mesh size of thousands of millions of elements. Then, it seems necessary to conduct some kind of simplifications.

In this sense, the recent multi-scale computational efforts of Kannan et al. [17] showed promising results with a huge computational cost reduction. In their work, a Q3D method was able to predict the location and the magnitude of the inflammation using spirometry data [18]. Also, drug absorption, transport, and retention in the human lungs could be computationally obtained [19, 20] to see if the inflammation at the right location can be mitigated. These are very significant results in the context of not only the drug delivery, but also for the prediction of diseases, drug residence times and targeted drug delivery. In this regards, Kannan et al. [20, 21] have shown that modelling any cartilaginous ring structures would increase the depositions, partially due to enhanced vorticity.

Other methods combine both CFD calculations and experimental tests performed on realistic 3D models of the upper airways and of the bronchial tree, up to the 4^{th}-6^{th} generations. Elcner et al. [22] used CT scanners of the upper airways and tracheobronchial tree up to the 4^{th} generation in order to run numerical simulations of the inspiratory flow of air for a ventilation of 7.5 L/min (sedentary) and 15 L/min (deep breath). The predicted flow velocities were compared with experimental measurements obtained at several positions inside a model that was casted in silicone, for which Phase Doppler Anemometry (PDA) and seeding particles of size 3 μm were used. Yousefi et al. [23] also adopted CT scanners to

generate a realistic model of the lung from the mouth to the 6th level of the bronchial tree. CFD simulations were run in order to predict aerosol delivery from Surface Acoustic Wave (SAW) nebulizations with a distribution of particles ranging from 1 μm to 7.6 μm. A combined Eulerian-Lagrangian approach was used to calculate the dispersed phase for an air inflow of 30 L/min. The same methodology was reported in Mohammadian and Pourmehran [24], where magnetic drug delivery from SAW nebulizations was numerically investigated. Recently, Xu et al. [25] performed Particle Image Velocimetry (PIV) measurements on a scaled model of the upper airways and trachea obtained from Magnetic Resonance Imaging (MRI). The inspiratory and expiratory airflows were numerically simulated for three constant flow rates that were equivalent to 18, 32 and 45 L/min. The numerical results were then compared with PIV measurements collected inside the experimental model, which was made by borosilicate glass and photosensitive resin and seeded with particles of 1 μm in size. These investigations show helpful procedures and methodologies that can be adopted in order to generate realistic models of the upper airways and bronchial tree.

The present work is aimed at the extension of a realistic model [14, 26, 27] of the lower airways (conductive zone of the lung, from generation 0 to 16), which has been validated to reproduce the air-lung flow, towards particle deposition predictive capabilities. Based on the results obtained, the target of the present work is to characterize the particle deposition at each generation of the lung model, which has been additionally extended to include an elemental model of the upper airways (mouth, nose, pharynx and larynx) and also of the respiratory zone (generations 17 to 23).

2. Materials and Methods

The original model was developed from a single path that considers only one out of the two airways presented at each level, so that simulations were run within a reasonable computational cost. The effect of the truncated airway at each level was included in the calculations by means of a User-Defined Function (UDF) that obtains the velocity profile at each active (open) airway and then prescribes this profile as a boundary condition at the truncated airway (Figure 1). This was found very useful in order to simulate the operation of the truncated airways at each bronchiole.

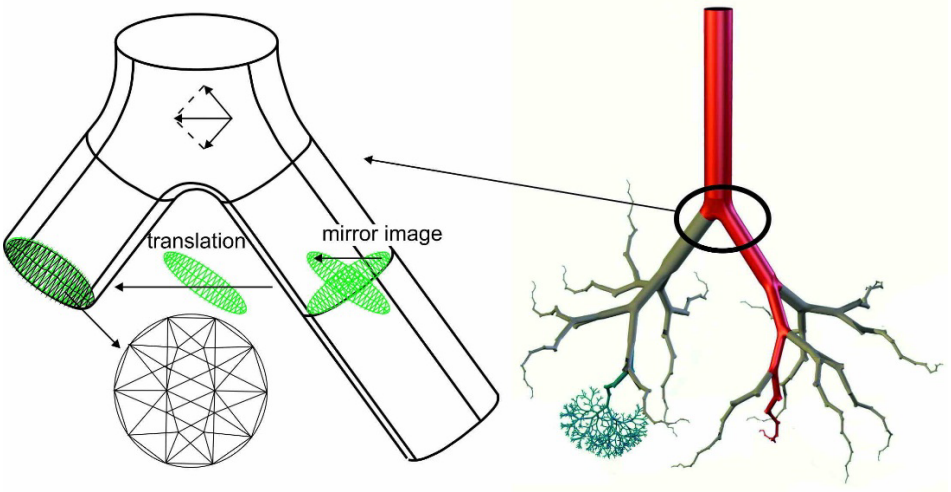

Figure 1. Layout of the construction of the lung model using an individual path.

The numerical model of the nasal cavity and nasopharynx zone was obtained from a 30 year-old woman by means of CT (Computed Tomography) images [28], while the throat reproduces the model reported in Brouns et al. [29]. According to the geometry that was previously described [26], the lung morphology follows the models reported in Weibel [15] and Kitaoka et al [16]. The full 3D geometry of the lung and upper airways has been developed with the commercial code ANSYS Gambit® [30]. The diameter of the trachea is 1.8 cm with a length of 12 cm, and the bifurcation angle was set to 35° (related to the main axis) according to the guidelines given in Fernández-Tena [14] and Fernández-Tena et al. [26]. The geometry of the bifurcations at the bronchus in all the generations was developed by a similar procedure.

Figure 2 shows a detail of the numerical model and of the mesh (about one million cells). A boundary layer mesh was previously built before meshing the whole model in order to obtain a better description of the flow close to the walls. The used algorithm in this boundary layer was:

- Aspect ratio first
- First percent (a/w): 10%
- Growth factor (b/a): 1.2
- Rows: 6
- Last percent (c/w): 24.88%

The lung model was meshed with tetrahedral cells since this type of cells can be better adapted to complex geometries. The size of the tetrahedrons, which was reduced while descending from the high order to the low order generations, is consistent with the size of the boundary layer cells. The volume of the cells ranges between $2.96 \cdot 10^{-12}$ and $2.01 \cdot 10^{-10}$ m^3. The maximum equiangle skew was restricted to 0.6 for 97.60% of the cells in the mesh, thus showing a low degree of cell deformation.

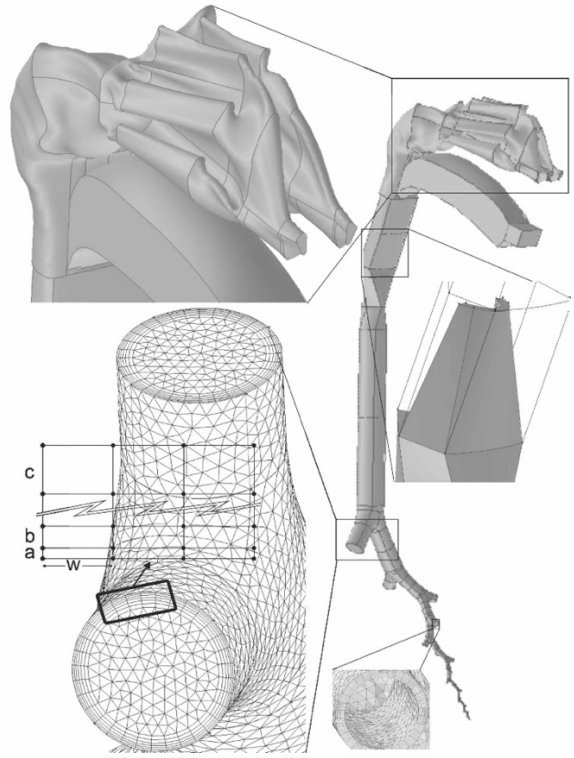

Figure 2. Numerical model: details of nose, epiglottis and mesh type (boundary layer with structured mesh and tetrahedral cells for volume meshing).

Additional meshes of size $2 \cdot 10^6$ and $4 \cdot 10^6$ cells were generated in order to investigate the sensitivity of the numerical calculations respecting the size of the mesh. It was found that the change in the outlet static pressure was not very significant, resulting in relative differences of 1.45% and 1.02% for the meshes of $1 \cdot 10^6$ and $2 \cdot 10^6$ cells respectively when compared to the finest mesh of $4 \cdot 10^6$ cells.

The numerical simulations were performed with the commercial code ANSYS Fluent® [31]. This code was used to solve the full steady 3D Reynolds-Averaged Navier-Stokes equations (RANS) by the finite volume method. The fluid used in the calculations was air (with constant density of 1.225 kg m^{-3} and dynamic viscosity of $1.7894 \cdot 10^{-5}$ kg $(m\ s)^{-1}$). The mean velocity magnitude at the trachea ranges between 0.65 m s^{-1} and 3.93 m s^{-1}, which brings about a variation of the Reynolds number between 840 and 5050. The model used for turbulent closure was the SST k-ω in order to effectively address both laminar and turbulent flow conditions, together with the transitional flows option that enables a low-Reynolds number correction to the turbulent viscosity. This model provides a good approximation to transitional flows because the magnitude of ω does not reach the zero value as the laminar flow limit is approached. Furthermore, turbulence is

simulated all the way to the viscous sublayer thus avoiding the use of standard wall functions, which are inaccurate for transitional flows. The coupling between pressure and velocity fields was established by means of the SIMPLE algorithm. Second-order upwind discretization was used for the convection terms and central difference discretization was established for the diffusion terms. The $y+$ value at any wall boundary was kept in the order of 2 or less. This numerical model had already been tested in previous works: Fernández-Tena [14], Fernández-Tena et al. [26] and Pandal-Blanco et al. [27].

The flow of air through the lung airways during the process of breathing is induced by the pressure difference that is generated between the pharyngeal region (nose or mouth) and the alveolar sacs. The air (and also any existing particle) is inhaled as a result of the depression produced by the stretch of the alveolar sacs, while the opposite effect takes place during exhalation: the alveolar sacs contract thus causing a higher pressure than that existing at the atmosphere. A single pressure boundary condition would be therefore required during a CFD calculation in order to reproduce this situation in a realistic way, since pressure variations at the outlet are induced by the deformation of the alveolar sacs. However, this deformation is replaced in practice by a boundary condition that prescribes a static pressure either below (inhalation) or above (exhalation) atmospheric conditions as the generated effect. Thus, a specific flow rate at the mouth and a constant gauge pressure at the lowest generation were imposed as boundary conditions. Additionally, a User-Defined Function (UDF) was included in the code in order to prescribe a symmetric operation of the two branches at each bronchus. A detailed description of this UDF (about 400 lines long) can be found in [14, 26, 27]. Essentially, this UDF acquires the velocity profile at each open branch from the numerical calculations and then specifies the same profile at the equivalent truncated branch. This procedure is repeated iteratively during the calculations until the convergence of the flow field is achieved, when scaled residuals for continuity and momentum equation reached a magnitude of 10^{-5}.

Particle trajectory equations can be either solved together with the equations for the continuum flow (coupled) or once the equations of the flow have converged (uncoupled). The uncoupled option was chosen for the present case. Hence, once the steady simulations had finished, the Discrete Phase Model (DPM) was triggered in order to predict the trajectory of discrete phase particles. This model uses an Euler-Lagrange approach, where the fluid phase is considered as a continuum by solving the Navier-Stokes equations while the dispersed phase is calculated by tracking a large number of particles through the flow field that was previously determined. The particles are supposed as inert and the influence of the Brownian motion, induced by the collision of the air molecules, is negligible, since drag force is usually the dominant force because of the difference between the density of the particles and that of the fluid. The stochastic tracking option was selected inside this model in order to include the effect of turbulence in the particle dispersion. Particle trajectories were then calculated within the steady flow fields of interest as a post-processing step. Particles were introduced by means of an injection-type surface, where velocity and particle properties were established. A random walk method was applied to reproduce the effect of turbulent fluctuations on particle motion. In a previous work [32], some authors found that 50,000 particles are usually required to minimize random variations of the deposition efficiency predictions due to the randomness of the particle

position profile. The tracking parameters used were 5,000 for the ‘maximum number steps’ and 5 for the ‘step length factor’. Deposition is determined by computing the ‘trapped’ particles when their center of mass touches the walls. Also, the code can report the number of incomplete, aborted, or untracked particles, which can be minimized by adjusting the input parameters.

3. Results

The tested flow rates were 18, 30 and 75 L min^{-1}, which are equivalent to different respiratory rates varying from light activity to heavy exercise. The latter value lies within the range observed during forced inhalations (as in the case of drug intake), where the maximum inhaled flow can reach a magnitude in the order of 100 L min^{-1} according to the bibliography. The seeding conditions of the particles were:

- Inert material density: 1000 kg m^{-3}
- Particle size: 0.5 μm, 1 μm, 3.1 μm, 5.7 μm, 10 μm, 15 μm, 20 μm and 25 μm
- Velocity: that of the air flow
- Density: 0.3%
- Number of injected particles: 2,471,642

The regional deposition of particles is quantified in terms of the Deposition Fraction (DF), defined as the mass ratio of deposited particles in a specific generation to the particles entering the lung.

$$\mathrm{DF} = \frac{\text{deposited particles in a generation}}{\text{particles entering the lung}}$$

Figure 3 presents the spatial distribution of the Deposition Fraction as a function of the position in the bronchial tree (branch number) and of the size of the inhaled particles. The three respiratory rates simulated are shown. The label 'OP' in the bottom axis means 'OroPharynx' and number '0'represents the trachea. Thus, values of the DF higher than zero in the range between 1 and 23 represents particles that have reached the bronchial tree. It can be seen in figure 3 that a larger amount of particles tends to accumulate inside the oropharyngeal region and also inside the first generations of the respiratory tract as the flow rate increases. The same effect is observed when increasing the particle size, which is especially noticeable at the highest flow rate. Thus, according to the results shown in this figure, the use of inhalers with particles larger than 15 μm and flow rates over 30 L min^{-1} should be avoided, since the amount of deposited particles before they can reach the lung is in the order of 50%-70%, reaching a magnitude close to 99% at the highest flow rate for the size of 20 μm and 25 μm. In contrast, for a size lower than 15 μm only about 20%-30% of the inhaled particles are deposited in the upper airways.

The results shown in figure 3 should be considered as average values, since they were obtained by assuming a constant inflow of air. Obviously, the flow during a forced inhalation is not constant, but it is typically observed that the larger amount of particle deposition takes place during the initial moments of the inhalation, where the flow of air reach the higher values. Therefore, the results of this figure can be used to limit the maximum transient flow of air that allow the particles of a specific size to reach the lower levels of the lung.

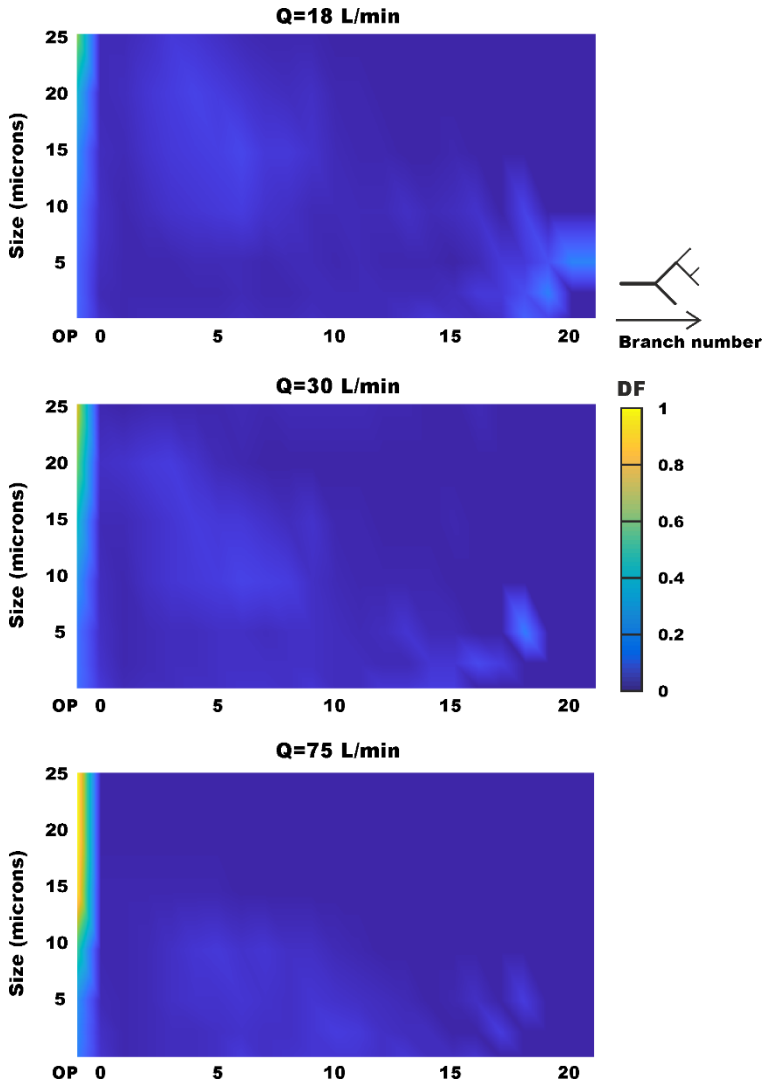

Figure 3. Deposition Fraction (DF) in the airways as a function of the size of the inhaled particles at three respiratory rates.

As a more detailed example of the pattern of deposition, figure 4 shows the concentration (kg m^{-2}) of the particles collected on the lung walls for a flow rate of 30 L min^{-1} and a particle size of 15 μm. In this figure, the red color shows high concentration of particles on the walls, whereas the blue color means absence of collected particles. As can be seen, most of the particles are accumulated in the upper airways, mainly at the mouth and also at the confluence of the larynx and the trachea (epiglottis), while the remaining particles travel across the lung. In addition, it is observed that the evacuation of the particles at the truncated branches was successfully simulated by means of the UDF, and therefore it can be concluded that the explained procedure allowed simulating the operation of the entire lung by means of a single individual path.

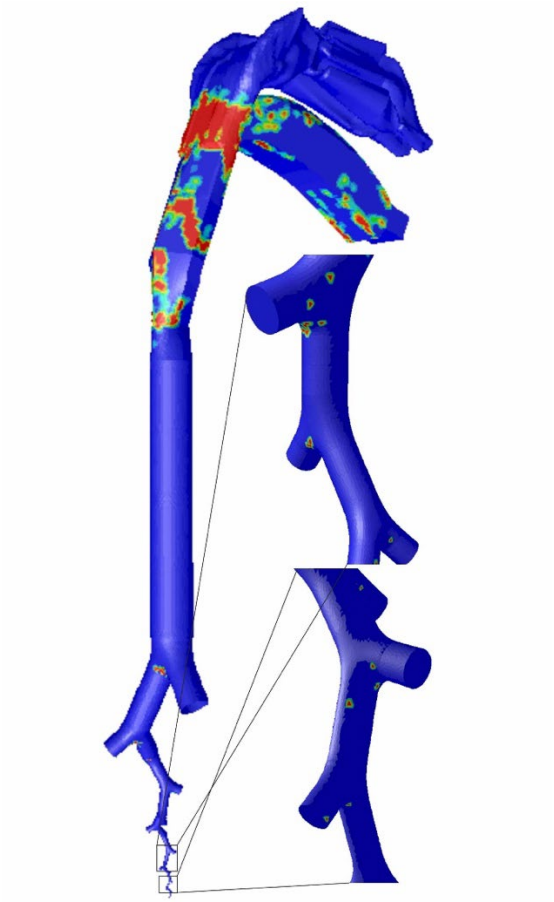

Figure 4. Particle concentration (kg m^{-2}) for a size of 15 μm and a flow rate of 30 L min^{-1}.

4. Discussion

The results shown in the previous section agree with those found in Dolovich and Newhouse [33], where it was concluded that fine particles are collected inside the peripheral airways whereas coarse particles are chiefly deposited inside the upper respiratory tract. A better contrast of the numerical predictions can be carried out by using the results presented in Conway et al. [34] and Katz et al. [35], where the aerosol deposition fraction in the respiratory tract of healthy human subjects (six males between 20 and 31 years old) was investigated by 2D and 3D imaging methods. The conditions of these tests were:

- Tidal volume: 1000 mL
- Inhalation time: 3.33 s
- Particle size: 3.1 and 5.7 μm
- Mean flow rate: 18 L min^{-1}

The Deposition Fraction at each generation in the experimental tests of Conway et al. [34] was estimated from a theoretical lung model (additional details on the model are shown in the paper). The experimental uncertainty regarding the Volume Median Diameter (VMD) of the particles is about ±7% for the size of 3.1 μm and about ±14% for the 5.7 μm particles, according to the data provided in reference [34].

A comparison between these experimental results and the data predicted with the CFD code is presented in Figure 5, where the whole particle sizes simulated are also shown. The Deposition Fraction in this figure is based on the particles that reach the trachea (level 0), thus excluding those particles that were previously collected in the oropharynx according to the results shown in figure 3. The numerical results were obtained for an intake of air of 18 L min^{-1} in order to be compared with the tests of Conway et al. [34] for a particle size of 3.1 μm and 5.7 μm. Additionally, Figure 5 also includes the numerical predictions reported in Deng et al. [36] for an inflow of 18 L·min^{-1} that was seeded with particles of density 1000 kg/m^3 and size ranging from 0.5 μm to 10 μm.

As seen in figure 5, in accordance with the previous results presented in figure 3, the finer particles (up to a size of 15 μm) are mainly collected in the lowest levels of the lung, showing a maximum magnitude of the deposition fraction that ranges from 20% to 40% and it is typically observed below level 16. Besides the general trends observed, the magnitude of the DF predicted by the numerical model is very close to the values reported in reference [34], showing relative differences close to 5% for the maximum magnitude of the Deposition Fraction. The only relevant difference observed is related to the generation where the maximum DF is predicted: the model predicts maximum DF at level 20 whereas the data of Conway et al. [34] shows maximum particle concentrations at generation 19. In this regard, the main differences between the CFD calculations and the experiments that are seen in this figure may be due to the numerical models used to estimate the geometry of the lung or, additionally, due to the initial parameters imposed.

Similar trends are observed between the results obtained with the present numerical model and the predictions reported in reference [36], showing

maximum magnitudes of the DF that are always located between levels 19 and 20 for particle sizes below 10 μm. In this case, however, the maximum magnitudes of the DF observed at the last generations are lower than those reported in [34] for the size 3.1 μm and 5.7 μm, which can be partially explained by the fact that the actual particle sizes simulated in [36] were 3 μm and 5 μm. There is a general good agreement between the predictions of the actual model and the simulations of Deng et al. [36] for the sizes 0.5 μm and 1 μm, although it is seen that the maximum DF is not predicted at the same generation. Finally, it is observed that the agreement is especially good for the particles of size 10 μm, where the deposition by impaction seems to be the dominant phenomenon.

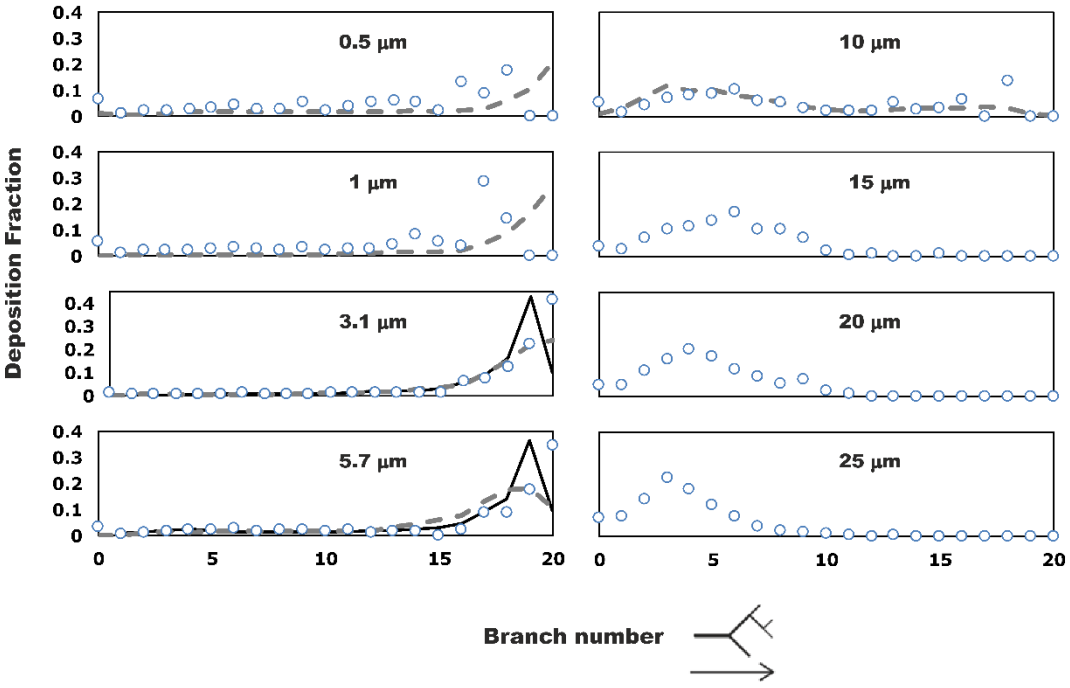

Figure 5. Deposition Fraction as a function of the particle size and of the position in the bronchial tree at 18 L min^{-1}. Comparisons with the experimental results obtained in Conway et al. [34] (solid lines) and with the numerical results from Deng et al. [36] (dashed lines) are also shown.

Finally, when the particle size increases above 15 μm it is observed that a higher percentage of particles is collected in the upper generations of the bronchial tree. Specifically, the CFD calculations predict that near 86%-96% of the particles remain above the 8th generation, with maximum values of the DF predicted between levels 4-6.

To sum up, the results presented in this paper showed that, with a convenient lung morphology and a proper boundary condition that prescribes symmetric operation at each branch, Computational Fluid Dynamic techniques can be a valuable tool in order to estimate the deposition of inhaled particles in the human airways, thus avoiding complex laboratory tests that usually require volunteers to be exposed to radiation.

5. Conclusions

This paper has explored a general methodology to simulate particle deposition in a model of a human lung that follows the geometries of Weibel [15] and Kitaoka et al. [16]. The model includes a full characterization of the lower conductive zone of the lung (generations 0 to 23) that could be simulated within reasonable computational times. Due to the high number of branches it was necessary to adopt a single pathway for the numerical calculations, so that the boundary conditions applied at the truncated branches were of special relevance. In this sense, the operation of the 'truncated' airways was considered in the simulations by means of a User-Defined Function (UDF). This function was used to: *i)* obtain the velocity profile at each 'active' (open) branch, and *ii)* specify the same profile at the truncated branch, cell by cell. This was found very useful in order to simulate the operation of the truncated branches at each bronchiole. The obtained results proved a very good agreement with experimental data obtained by previous researching groups, thus showing that the reported model can provide a realistic description of the operation of the lung while avoiding too large computational costs.

It must be noted, however, that the numerical model presented in this paper is a simplified geometry of the bronchial tree since it cannot discriminate between the left and right lung, which would be a desirable feature due to the inherent asymmetry of the pulmonary system. Our future efforts will be focused on building a more realistic model of the first generations of the lung (down to levels 3-4, since the main asymmetries are observed at these first levels) from Computer Tomography images in order to combine this realistic model with the single-path geometry described in this paper. The combined model could then be used to simulate the operation of the lung until 23th generation while being able to discern between the flow of air towards either the left or the right lung.

Acknowledgements

Authors acknowledge that this work was partially funded by the Spanish Ministry of Economy, Industry and Competitiveness – Instituto de Salud Carlos III, under Project "Estudio de la influencia de la geometría de las vías respiratorias en las patologías pulmonares obstructivas (PI17/01639)", and was supported by Universidad de Oviedo under Projects "Desarrollo de nuevas metodologías de enseñanza: reconstitución digital de las vías aéreas humanas a partir de imágenes de tomografía computacional (PINN-17-A-044)" and "Desarrollo de nuevo material docente para prácticas de Anatomía humana (PINN-18-A-069)".

Author Disclosure Statement

The authors declare that no conflicts of interest exist.

References

[1] Anderson JO, Thundiyil JG, Stolbach A. Clearing the air: a review of the effects of particulate matter air pollution on human health. *J. Med. Toxicol*. 2012;**8**(2):166-175. doi: 10.1007/s13181-011-0203-1.

[2] Kumar P, Morawska L, Martani C, et al. Air pollution and lung cancer. *Cancer Detect. Prev.* 1982;5:371-374.

[3] Cordasco EM, VanOrdstrand HS. Air pollution and COPD. *Postgrad. Med.* 1977;**62**(1):124-127.

[4] Neher JO, Koenig JQ. Health effects of outdoor air pollution. *Am. Fam. Physician.* 1994;**49**(6):1397-404.

[5] Keller R. Air pollution and lung diseases in adults. *Sozial-und Praventivmedizin*. 1986;**31**(1):12-5.

[6] Ivey JW, Lewis D, Church T, Finlay WH, Vehring R. A correlation equation for the mass median aerodynamic diameter of the aerosol emitted by solution metered dose inhalers. *Int. J. Pharmaceut.* 2014;**465**(1-2):18-24. doi: 10.1016/j.ijpharm.2014.01.039.

[7] Pritchard JN. Particle growth in the airways and the influence of airflow. A new concept in inhalation therapy. *Bussum: Medicom.* 1987:3-24.

[8] Jackson W. Nebulised Budesonide *Therapy in Asthma: A Scientific and Practical Review*. Clinical Vision; 1995.

[9] Pharmacopeia on line. http://www.uspbpep.com/, Aerosols, Nasal Sprays, Metered-Dose Inhalers, and Dry Powder Inhalers. Webcom Limited: Toronto; 2006.

[10] Newman SP. Aerosol deposition considerations in inhalation therapy. *Chest.* 1985;**88**(2):152S-160S.

[11] Fernández-Tena A, Casan-Clarà P. Deposition of inhaled particles in the lungs. *Arch. Bronconeumol.* (English Edition), 2012;**48**(7):240-246. doi: 10.1016/j.arbres.2012.02.003

[12] Yang Y, Martonen T, Caillibotte G, Katz I, Sbirlea-Apiou G. Deposition Mechanics of Pharmaceutical Particles in Human Airways. *Inhalation Aerosols.* CRC Press;2006:27-56.

[13] Faure JP, Breque C, Danion J, Delpech PO, Oriot D, Richer JP. SIM Life: a new surgical simulation device using a human perfused cadaver. *Surg. Radiol. Anat.* 2017;**39**(2):211-217. doi: 10.1007/s00276-016-1715-9.

[14] Fernández-Tena A. Clinical applications of fluid dynamics models in respiratory disease. *PhD Thesis*. Spain: University of Oviedo; 2014.

[15] Weibel ER. *Morphometry of the Human Lung*. Berlin:Springer-Verlag; 1963.

[16] Kitaoka H, Takaki R, Suki B. A three-dimensional model of the human airway tree. *J. Appl. Physiol.* 1999;**87**(6):2207-2217. doi: /10.1152/jappl.1999.87.6.2207.

[17] Kannan R, Chen ZJ, Singh N, et al. A quasi-3D wire approach to model pulmonary airflow in human airways. *Int. J. Numer. Method. Biomed. Eng.* 2017;**33**(7). doi: 10.1002/cnm.2838.

[18] Kannan R, Singh N, Przekwas A. A quasi-3D compartmental multi-scale approach to detect and quantify diseased regional lung constriction using spirometry data. *Int. J. Numer. Method. Biomed. Eng.* 2018;**34**(5). doi: 10.1002/cnm.2973.

[19] Kannan R, Singh N, Przekwas A. A compartment-quasi-3D multiscale approach for drug absorption, transport, and retention in the human lungs. *Int. J. Numer. Method. Biomed. Eng.* 2018;**34**(5). doi: 10.1002/cnm.2955.

[20] Kannan R, Przekwas AJ, Singh N, Delvadia R, Tian G, Walenga R. Pharmaceutical aerosols deposition patterns from a Dry Powder Inhaler: Euler Lagrangian prediction and validation. *Med. Eng. Phys.* 2017;**42**:35-47. doi: 10.1016/j.medengphy.2016.11.007.
[21] Kannan R, Guo P, Przekwas A. Particle transport in the human respiratory tract: formulation of a nodal inverse distance weighted Eulerian–Lagrangian transport and implementation of the Wind–Kessel algorithm for an oral delivery. *Int. J. Numer. Method. Biomed. Eng.* 2016;**32**(6). doi: 10.1002/cnm.2746.
[22] Elcner J, Lizal F, Jedelski J, Jicha M, Chovankova M. Numerical investigation of inspiratory airflow in a realistic model of the human tracheobronchial airways and a comparison with experimental results. *Biomech. Model. Mechanobiol.* 2016;**15**(2):447-469. doi: 10.1007/s10237-015-0701-1.
[23] Yousefi M, Pourmehran O, Gorji-Bandpy M, Inthavong K, Yeo L, Tu J. CFD simulation of aerosol delivery to a human lung via surface acoustic wave nebulization. *Biomech. Model. Mechanobiol.* 2017;**16**(6):2035–2050. doi: 10.1007/s10237-017-0936-0.
[24] Mohammadian M, Pourmehran O. CFPD simulation of magnetic drug delivery to a human lung using an SAW nebulizer. *Biomech. Model. Mechanobiol.* 2019;**18**(3):547–562. doi: 10.1007/s10237-018-1101-0.
[25] Xu X, Wu J, Weng W, Fu M. Investigation of inhalation and exhalation flow pattern in a realistic human upper airway model by PIV experiments and CFD simulations. *Biomech. Model. Mechanobiol.* (in press). doi: 10.1007/s10237-020-01299-3.
[26] Fernández-Tena A, Fernández J, Álvarez E, Casan P, Walters DK. Design of a numerical model of lung by means of a special boundary condition in the truncated branches. *Int. J. Numer. Method. Biomed. Eng.* 2017;**33**(6). doi: 10.1002/cnm.2830.
[27] Pandal-Blanco A, Barrio-Perotti R, Agujetas-Ortiz R, Fernandez-Tena A. Implementation of a specific boundary condition for a simplified symmetric single-path CFD lung model with OpenFOAM. *Biomech. Model Mechanobiol.* 2019;**18**(6):1759-1771. doi: 10.1007/s10237-019-01174-w.
[28] Ruiz PC, Ruiz FC, López AC, Español CC. Computational fluid dynamics simulations of the airflow in the human nasal cavity. *Acta Otorrinolaringol. Esp.* 2005;**56**(9):403-410.
[29] Brouns MS, Jayaraju T, Lacor C, et al. Tracheal stenosis: a flow dynamics study. *J. Appl. Physiol.* 2007;**102**(3):1178-1184.
[30] ANSYS Gambit, version 2.4.6. (2006) ®ANSYS Inc.
[31] ANSYS Fluent, version 18.2 (2017) ®ANSYS Inc.
[32] Robinson RJ, Oldham MJ, Clinkenbeard RE, Rai P. Experimental and numerical smoke carcinogen deposition in a multi-generation human replica tracheobronchial model. *Ann. Biomed. Eng.* 2006;**34**(3):373-383.
[33] Dolovich MB, Newhouse MT. Aerosols. Generation, methods of administration, and therapeutic applications in asthma. In: *Allergy Principles and Practice*. St Louis: Mosby Year Book Inc; 1993:712–739.
[34] Conway J, Fleming J, Majoral C, et al. Controlled, parametric, individualized, 2-D and 3-D imaging measurements of aerosol deposition in the respiratory tract of healthy human subjects for model validation. *J. Aerosol Sci.* 2012;**52**:1-17. doi: /10.1016/j.jaerosci.2012.04.006.

[35] Katz I, Pichelin M, Caillibotte G, et al. Controlled, parametric, individualized, 2D, and 3D imaging measurements of aerosol deposition in the respiratory tract of healthy human subjects: Preliminary comparisons with simulations. *Aerosol Sci. Tech.* 2013;**47**(7):714-723. doi: 10.1080/02786826.2013.784393.
[36] Deng Q, Deng L, Miao Y, Guo X, Li Y. Particle deposition in the human lung: Health implications of particulate matter from different sources. *Environ. Res.* 2019;**169**:237-245. doi: 10.1016/j.envres.2018.11.014.